Influence of nitrogen dose on the charge density of nitrogen-implanted buried oxide in SOI wafers

Zheng Zhongshan(郑中山)[1,2,†], Liu Zhongli(刘忠立)[2], Li Ning(李宁)[2], Li Guohua(李国花)[2], and Zhang Enxia(张恩霞)[3]

(1 Department of Physics, University of Jinan, Jinan 250022, China)
(2 Institute of Semiconductors, Chinese Academy of Sciences, Beijing 100083, China)
(3 College of Material Engineering, Shanghai University of Engineering Science, Shanghai 201620, China)

Abstract: To harden silicon-on-insulator (SOI) wafers fabricated using separation by implanted oxygen (SIMOX) to total-dose irradiation, the technique of nitrogen implantation into the buried oxide (BOX) layer of SIMOX wafers can be used. However, in this work, it has been found that all the nitrogen-implanted BOX layers reveal greater initial positive charge densities, which increased with increasing nitrogen implantation dose. Also, the results indicate that excessively large nitrogen implantation dose reduced the radiation tolerance of BOX for its high initial positive charge density. The bigger initial positive charge densities can be ascribed to the accumulation of implanted nitrogen near the Si-BOX interface after annealing. On the other hand, in our work, it has also been observed that, unlike nitrogen-implanted BOX, all the fluorine-implanted BOX layers show a negative charge density. To obtain the initial charge densities of the BOX layers, the tested samples were fabricated with a metal-BOX-silicon (MBS) structure based on SIMOX wafers for high-frequency capacitance–voltage (C–V) analysis.

Key words: buried oxide; charge density; nitrogen implantation; fluorine implantation
DOI: 10.1088/1674-4926/31/2/026001 **PACC:** 7340Q; 6170T

1. Introduction

Silicon-on-insulator (SOI) CMOS devices have advantages over their bulk counterparts for single event upset and dose rate transient upset effects due to their small charge-collection volume and p–n junction area[1,2]. However, the buried layer of SOI wafers reduces the total-dose radiation tolerance of SOI devices[3,4]. Radiation-induced positive charges trapped in the buried layer can lead to the increase of leakage current and even failure for SOI devices. Therefore, improvement of the total-dose radiation hardness of the buried layers for space application of SOI technology has become more and more important, and many hardening techniques have been proposed. Barchuk *et al.* fabricated a hardened SOI structure with multilayer buried dielectric, SiO_2–Si_3N_4–SiO_2, by the ZMR-technique[5]. Yi *et al.* prepared a type of SOI material by oxygen and nitrogen ion implantation to enhance the radiation tolerance of devices[6]. For separation by implanted oxygen (SIMOX) SOI wafers, Yang *et al.* researched the hardening method of silicon implantation into buried oxide (BOX)[7]. In particular, the technique of nitrogen implantation into BOX has been studied for hardening SIMOX materials[8–10], and the BOX processed properly by nitrogen ion implantation really revealed an improved radiation hardness. Although the nitrogen ion implantation dose is obviously an important factor in the BOX's behavior, so far there have been no reports on the effect of nitrogen dose on the properties of SIMOX wafers, in particular the initial charge density of nitrogen-implanted BOX, except for their radiation hardness. On the other hand, this initial charge density should be considered a very important parameter for hardening SIMOX wafers by nitrogen implantation, because a higher initial positive charge density probably causes a leakage current for SOI n-channel devices, similar to a radiation-induced total dose response. Therefore, it is necessary to properly understand the relationship between nitrogen implantation doses and initial charge densities to choose the right implantation conditions to harden SIMOX wafers better.

In this work, we focus on the dependence of the initial positive charge densities of nitrogen-implanted BOX layers on nitrogen implantation doses. So, nitrogen ions were implanted into the BOX of SIMOX wafers at the same energy at three very different doses. The tested capacitor samples with a metal–BOX–silicon (MBS) structure were fabricated by removing the top silicon layer of the SIMOX wafers for capacitance–voltage (C–V) measurement. According to the high-frequency C–V curves of these MBS capacitors, the effective initial positive charge densities of the nitrogen-implanted BOX layers were calculated and discussed. In addition, fluorine ions were implanted into another group of SIMOX wafers in our previous work. Fluorine-implanted MBS capacitors were also fabricated, and their preliminary C–V results were compared with those of the nitrogen-implanted capacitors.

2. Experiment

First, oxygen ions were implanted into p-type (100) silicon wafers, according to the dose-energy match obtained by Chen *et al.*[11]. During implantation, the substrate was at 650 °C. Following implantation, annealing was carried out at 1300 °C for 5 h. The formed SIMOX wafers have a BOX layer of about 150

† Corresponding author. Email: ss_zhengzs@ujn. edu. cn
Received 27 August 2009, revised manuscript received 27 September 2009

Table 1. Effective charge densities of the BOX layers of the MBSn0#–3# capacitors.

Capacitor	Nitrogen dose (cm^{-2})	C_{BOX} (pF)	V_{FB} (V)	N_{eff} (cm^{-2})	Average N_t (cm^{-2})
MBSn0# -1	0	100	−0.5	-1.27×10^{11}	-1.26×10^{11}
MBSn0# -2	0	102	−0.5	-1.30×10^{11}	-1.26×10^{11}
MBSn0# -3	0	96	−0.5	-1.22×10^{11}	-1.26×10^{11}
MBSn1# -1	2.5×10^{15}	104	−1.1	0.662×10^{11}	0.682×10^{11}
MBSn1# -2	2.5×10^{15}	107	−1.1	0.682×10^{11}	0.682×10^{11}
MBSn1# -3	2.5×10^{15}	110	−1.1	0.701×10^{11}	0.682×10^{11}
MBSn2# -1	7.5×10^{15}	98	−2.2	4.06×10^{11}	4.04×10^{11}
MBSn2# -2	7.5×10^{15}	99	−2.2	4.10×10^{11}	4.04×10^{11}
MBSn2# -3	7.5×10^{15}	104	−2.2	3.97×10^{11}	4.04×10^{11}
MBSn3# -1	2.0×10^{16}	108	−9.0	27.9×10^{11}	26.0×10^{11}
MBSn3# -2	2.0×10^{16}	95	−8.5	23.0×10^{11}	26.0×10^{11}
MBSn3# -3	2.0×10^{16}	105	−9.0	27.1×10^{11}	26.0×10^{11}

nm and a 190 nm top Si layer. Then, nitrogen ions were implanted into the BOX layers of the fabricated SIMOX wafers at three different doses, 2.5×10^{15}, 7.5×10^{15} and 2.0×10^{16} cm^{-2}, respectively, at 90 keV. During the nitrogen implantation, the wafers were maintained at 300 °C. The subsequent annealing was performed at 1200 °C for 2 h in N_2 ambient.

For another group of standard SIMOX wafers with a 200 nm top Si layer, fluorine ions were implanted into their 380 nm BOX layers using 1×10^{15}, 2×10^{15} and $4\times10^{15}cm^{-2}$ doses, respectively, at 140 keV. After implantation, 900 °C 2 h annealing followed in N_2 ambient.

Last, MBS capacitors were fabricated on the implanted SIMOX wafers after the top Si layers were removed by the reactive-ion etching technique for C–V characterization.

The nitrogen-implanted capacitors were divided into three groups denoted by MBSn1#, n2#, and n3#, corresponding to the three doses 2.5×10^{15}, 7.5×10^{15} and 2.0×10^{16} cm^{-2}, respectively. In addition, MBSn0# as a control group was fabricated on a non-implanted SIMOX wafer. Similarly, the fluorine-implanted capacitors were denoted by MBSf1#, f2#, and f3#, corresponding to the ascending three doses, and the MBSf0# expressed the non-implanted capacitors. All the capacitors had an Al-gate area of 1.96×10^{-3} cm^2 by vacuum evaporation. At room temperature, the high-frequency C–V characteristics of the capacitor samples were obtained by a computer-controlled HP4275 LCR meter at 1 MHz.

3. Results and discussion

Figure 1 shows the typical high-frequency C–V curves of the MBS capacitors for each of the nitrogen-implanted groups. It is obvious that all the C–V curves of the implanted capacitors have the negative parallel shifts along the gate voltage axis, compared to the non-implanted control capacitor, and the greater the nitrogen implantation dose is, the greater the shift. The effective charge densities corresponding to the different capacitors can be extracted from the obtained C–V curves. According to the C–V theory, the high-frequency total capacitance C of an MBS capacitor is a series combination of the BOX capacitance C_{BOX} and the substrate depletion-layer capacitance C_s. Thus, the flat-band capacitance C_{FB} of the MBS capacitor can be calculated by

$$C_{FB}=C_{BOX}C_{sFB}/(C_{BOX}+C_{sFB}), \tag{1}$$

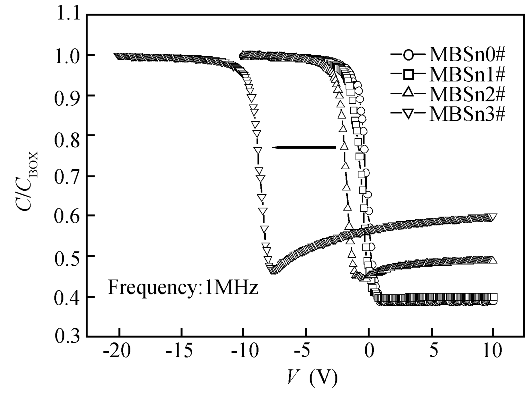

Fig. 1. Typical high-frequency C–V curves of the MBSn0#–n3# capacitors at 1 MHz.

where C_{sFB} is the flat-band capacitance of the Si substrate. With the C_{FB} obtained, the effective charge density in flat-band case, N_{eff}, is given by[12]

$$N_{eff}=(\Phi_{ms}-V_{FB})C_{BOX}/qS, \tag{2}$$

where Φ_{ms} is the potential difference corresponding to the work function difference between gate metal and substrate silicon, q is the elementary charge, and S is the gate area of the capacitor.

The N_{eff} values of the nitrogen-implanted capacitors are summarized in Table 1. By comparing the effective charge densities of the BOX layers of the different groups, it can be stated that the nitrogen implantation dose plays an important role in the changes of positive charge density. All the nitrogen-implanted samples have a positive N_{eff}, and N_{eff} increases with increasing nitrogen implantation dose. Nevertheless, there is no simple linear correlation between the nitrogen doses and the N_{eff} increments relative to the control, as seen in Table 1. The analysis shows that the N_{eff} increment exhibits an approximately exponential increase with dose.

It is well known that both fixed charges in BOX and interface-trapped charges at the Si-BOX interface contribute to V_{FB}; therefore, N_{eff} comprises the fixed charge density N_f and the interface-trapped charge density N_{it}, i.e.

$$N_{eff}=N_f+N_{it}. \tag{3}$$

The fixed charges give rise to only parallel shifts of C–V curves along the gate voltage axis, while the interface-trapped

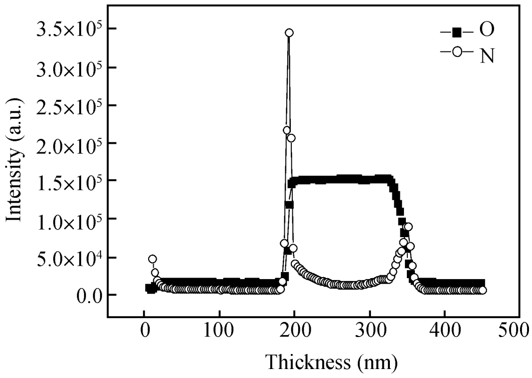

Fig. 2. Nitrogen and oxygen depth profiles of the SIMOX wafer into which 4×10^{15} cm^{-2} nitrogen ions were implanted at 90 keV and treated with 4 h 1200 °C annealing.

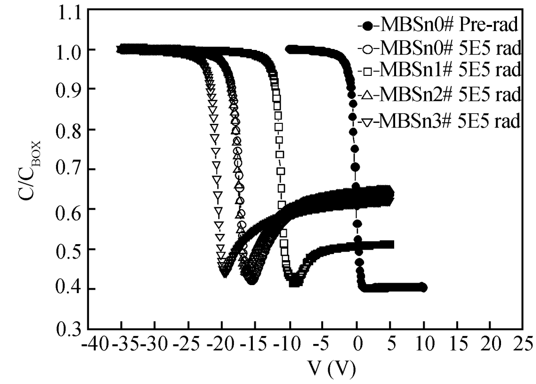

Fig. 3. High-frequency C–V curves of the nitrogen-implanted MBSn1#–3# capacitor after 5×10^5 rad(Si) irradiation and that of the control MBSn# capacitor pre- and post-irradiation.

charges distort the C–V curves due to the variation of N_{it} with the silicon surface potential as a function of gate voltage. From Fig. 1, there is no perceivable distortion induced by the interface-trapped charges for the C–V curves of MBSn1#–3#, compared with MBSn0#, except for a parallel shift. This indicates that the effect of the interface-trapped charges is negligible. Therefore, the value of N_{eff} is approximately equal to that of N_{f} (fixed charge density), and the shift of the C–V curves basically stems from the fixed charges in the BOX layers.

For thermal SiO_2, there are oxide fixed charges near the Si–SiO_2 interface, generally attributed to excess Si ions near the interface due to the lack of oxygen. Also, it has been found that there is a nitrogen accumulation near the Si–SiO_2 interface of the thermal SiO_2 prepared by oxidizing at high temperature and annealing in N_2, and an increasing fixed charge density has been observed[13]. For nitrogen-implanted SIMOX wafers, the existence of a nitrogen-rich region near the Si–BOX interface has been shown by the SIMS analysis in Fig. 2. So, compared with the non-implanted BOX, the greater positive charge density of the implanted BOX can be explained by a nitrogen-induced effect in the BOX side near the Si–BOX interface, which possibly prevents the combination of silicon and oxygen and causes an increase of excess Si ions. As a result, the greater the nitrogen implantation dose is, the more excess Si ions there are, and, consequently, the higher the positive charge densities are.

As for the abnormal kink phenomena in the region of strong inversion for the C–V curves of MBSn2# and n3# in Fig. 1, it can be explained by lateral spreading, beyond the gate area, of the surface inversion layer of the Si substrate[12], which is caused by the high positive charge density in BOX. That is, the spread inversion layer provides more minority carriers (i.e. electrons) than a normal one does, enlarging the effective gate area and increasing the Si surface capacitance. A larger flat-band voltage shift means a greater fixed charge density and more minority carriers in the spread inversion layer, leading to a larger Si surface capacitance. Therefore, the kink of the C–V curves from the implanted samples intensifies with increasing nitrogen dose.

Figure 3 displays the high-frequency C–V curves of the MBSn0#–3# capacitors after a 5×10^5 rad(Si) dose of γ-ray irradiation. It is clear that the C–V curve of the MBSn1# capacitor has the lowest radiation-induced shift, compared with the control MBSn0# capacitor before irradiation. According to this, it can be said that the wafer with the nitrogen implantation dose of 2.5×10^{15}cm^{-2} has an improvement of radiation hardness. Also, the results indicate that an excessively large nitrogen implantation dose will reduce the radiation tolerance of wafers for their high initial positive charge densities. So, for hardening purposes, nitrogen implantation doses should be controlled within an appropriate range.

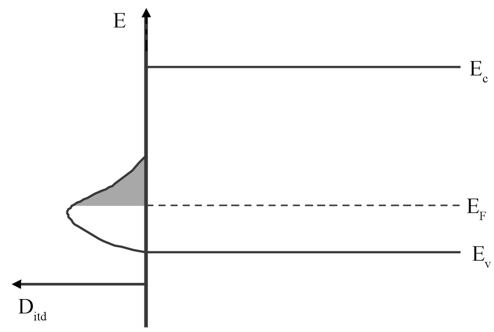

Fig. 4. Schematic illustration of the distribution of donor-like interface traps and the enery-band diagram for p-Si substrate in the flat-band case. The interface traps in the shaded area above the Fermi level E_{F} capture positive charges.

In contrast with MBSn1#–3#, MBSn0# has a negative effective charge density ($N_{\text{eff}} < 0$). According to the conventional model, donor-like interface trap levels are below the middle of the Si bandgap, hence the p-Si interface-trapped charge density N_{it} should be positive at flat-band. Figure 4 schematically illustrates the distribution of the donor-like interface trap density in the Si bandgap, with the symbols E_{C} and E_{V} denoting the bottom of the conduction band and the top of the valence band, respectively, and D_{itd} denoting the donor-like interface trap density. Seeing that the N_{eff} of MBSn0# is negative and the N_{it} positive, according to Eq. (3), the N_{f} of MBSn0# is negative. This indicates there are electron traps in the MBSn0# BOX, which were maybe introduced during removal of the top Si layers by reactive-ion etching.

The high-frequency C–V curves of the fluorine-implanted MBSf1#, f2#, and f3# capacitors display a positive shift along the gate voltage axis, compared to the non-implanted MBSf0#

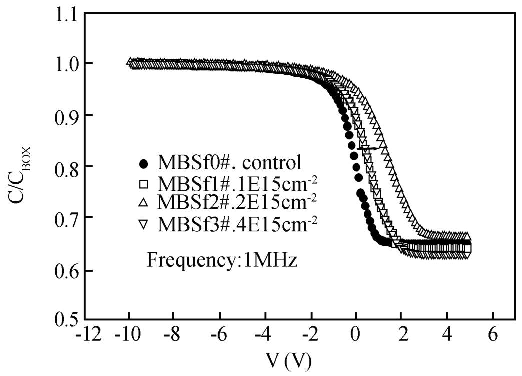

Fig. 5. High-frequency C–V curves of the MBSf0#–3# capacitors at 1 MHz.

capacitor, as shown in Fig. 5. This opposite shift to the nitrogen-implanted samples indicates that the effective charge density of the fluorine-implanted BOX layers is negative, i.e. there are the electron traps in the BOX layer caused by fluorine implantation. So far, there have been no reports that fluorine implantation into SIMOX wafers can lead to a negative effective charge density of BOX layers. On the other hand, unlike the nitrogen-implanted BOX, the relationship between the C–V shift and the fluorine implantation dose appears complex from Fig. 5. A reasonable explanation needs further research.

4. Conclusions

Nitrogen implantation in the SIMOX BOX layer caused an increase in its positive charge density, whereas fluorine implantation resulted in the increase of the negative charge density. For the nitrogen-implanted BOX layers, the bigger the nitrogen dose is, the greater the positive charge density. However, there is no such similar relation for the fluorine-implantation BOX layers, according to our preliminary work reported here. A detailed explanation about this needs further study. It is noticeable that, with a nitrogen implantation dose of 2.0×10^{16} cm^{-2}, the positive charge density significantly increases, which is ascribed to implanted nitrogen accumulation near the Si–BOX interface. Therefore, for hardening purposes, nitrogen dose should be limited to below 10^{16} cm^{-2}. On the other hand, in order to reduce the positive charge density, suppression of the nitrogen accumulation near the interface is also worth researching. In addition, because the fluorine-implanted BOX shows a negative charge density, the method of hardening SIMOX wafers using fluorine ion implantation deserves attention.

References

[1] Mikawa R E, Ackerman M R. Transient radiation effects in SOI static RAM cells. IEEE Trans Nucl Sci, 1987, 34(6): 1698

[2] Musseau O, Leray J L, Ferlet-Cavrois V, et al. SEU in SOI SRAMs — a static model. IEEE Trans Nucl Sci, 1994, 41(3): 607

[3] Schwank J R, Shaneyfelt M R, Dodd P E, et al. Correlation between Co-60 and X-ray radiation-induced charge buildup in silicon-on-insulator buried oxides. IEEE Trans Nucl Sci, 2000, 47(6): 2175

[4] Mayer D C. Modes of operation and radiation sensitivity of ultrathin SOI transistors. IEEE Trans Electron Devices, 1990, 37(5): 1280

[5] Barchuk I P, Kilchitskaya V I, Lysenko V S, et al. Electrical properties and radiation hardness of SOI systems with multilayer buried dielectric. IEEE Trans Nucl Sci, 1997, 44(6): 2542

[6] Yi W B, Zhang E X, Chen M, et al. Formation of total-dose-radiation hardened materials by sequential oxygen and nitrogen implantation and multi-step annealing. Semicond Sci Technol, 2004, 19(5): 571

[7] Yang Hui, Zhang Enxia, Zhang Zhengxuan. Effects of Si ion implantation on the total-dose radiation properties of SIMOX SOI materials. Chinese Journal of Semiconductors, 2007, 28(3): 323

[8] Zhang E X, Sun J Y, Chen J, et al. Radiation hardness improvement of separation by implantation of oxygen /silicon-on-insulator material by nitrogen ion implantation. Journal of Electronic Materials, 2005, 34(11): L53

[9] Zhang Enxia, Qian Cong, Zhang Zhengxuan, et al. Effect of nitrogen implantation technologies on total dose rad-hardness of SIMON materials. Chinese Journal of Semiconductors, 2005, 26(2): 1269

[10] Zhang Guoqiang, Liu Zhongli, Li Ning, et al. Effects of nitrogen on electrical characteristics of SIMOX devices. Chinese Journal of Semiconductors, 2005, 26(4): 835

[11] Chen M, Wang X, Chen J, et al. Dose-energy match for the formation of high-integrity buried oxide layers in low-dose separation-by-implantation-of-oxygen materials. Appl Phys Lett, 2002, 80: 880

[12] Nicollian E H, Brews J R. MOS (metal oxide semiconductor) physics and technology. New York: Wiley, 1982

[13] Pancholy R K, Erdmann F M. Radiation effects on oxynitride gate dielectrics. IEEE Trans Nucl Sci, 1983, 30(6): 4141